

Design and Development of a Laser Warning Sensor Prototype for Airborne Application

Tutul Gogoi* and Rajni Kumar

DRDO-Defence Geoinformatics Research Establishment, Chandigarh - 160 036, India

*E-mail: t.gogoi.k7@gmail.com

ABSTRACT

Due to recent developments in high-energy laser systems, the laser is becoming one of the most potential choices in battlefield applications. Laser of a laser range finder used to find target distance may be of nanosecond pulse width and a single pulse may be sufficient to gather the instantaneous range information. A laser target designator is a similar laser with higher energy and with programmable pulse repetition frequencies^{5,7}. Detection of such a specific battlefield laser radiation along with recognizing friend or foe is required for countermeasures. Designing a laser detection system that is capable of detecting such low-power level laser pulses of nanosecond pulse width at a long distance is a critical design and a challenging task. Again detecting a wide wavelength band that can start from 500 nm to around 1700 nm range using a single detector or device is also a challenging task. In this work, a sensor system is being designed and a prototype is developed to cover such a long band detection using a single detector for high-energy lasers. Also, in addition to detecting hostile code, the direction of an incoming laser beam is tried to incorporate into this sensor. The sensor can be utilized to detect unknown or non-friendly laser illumination from within a specific angular cone and distance.

Keywords: Angle of Arrival (AoA); Field Programmable Gate Array (FPGA); Laser Beam Rider (LBR); Laser Range Finder (LRF); Laser Target Designator (LTD); Pulse Repetition Frequency (PRF); Pulse Repetition Time (PRI); Type of Threat (ToT); Very High-Density Hardware Description Language (VHDL)

1. INTRODUCTION

Some of the determining key features of a laser are its narrow wavelength band, high peak power generation, working at the speed of light, laser beam conditioning like doing beam size modification and divergence reduction, etc. As a result of these features scientific and interactive analysis can be performed at a long distance remotely. There are multiple examples of such systems as laser spectroscopy, laser range finder, laser-based 3D mapping, laser target designation for bomb dropping, etc. In some of these applications, the laser detector can be on the laser source side itself, and in many applications may be towards the target side. In this work, a laser sensor is designed based on sensing incoming laser radiation for a range of wavelength from 500 nm to 1700 nm along with the direction of arrival. The system is designed with the capability of detecting pulsed laser signals with programmable pulse repetition frequencies, coming from systems like laser range finder, laser target designator, and laser beam rider devices. This kind of sensor can be developed and deployed in airborne platforms both commercial as well as defense, to detect such laser exposure threats. Subsequently, the threats can be mitigated and countermeasures can be taken.

One device would cover a specific direction of arrival of radiation as mentioned in table 1 and a few more such devices have to be installed judiciously on the aircraft to cover all the

Table 1. Laser parameters considered for design

Wavelength	1064 nm and 1540 nm (LRF)
	1064 nm (LTD)
	800 – 1100 nm (LBR)
Laser PRF	Range Finder: Single Shot
	Designator: 5-20 Hz
	Beam Rider: In a few kHz
Field of view	$\pm 45^\circ$ (Azimuth and Elevation)
Angular resolution	$\pm 2^\circ$

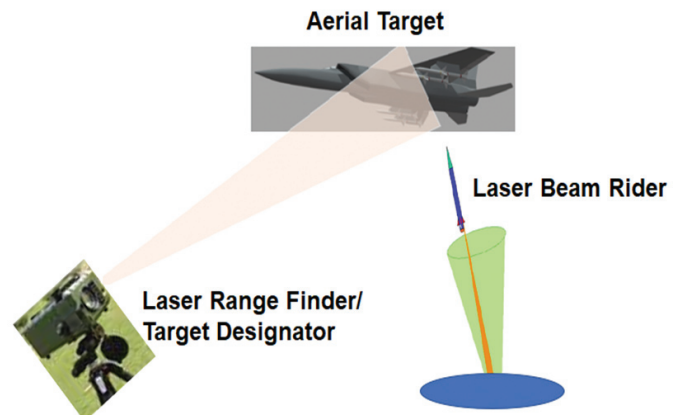


Figure 1. Different types of battlefield laser threats for an aerial target.

directions around it. The range of the range finder or designator can be quite large as high as 40 km due to the low divergence of the beam and high peak power. On the other hand, the beam divergence of a beam rider beam is quite large and hence the range is also less. The theoretical and design calculations presented here are approximate estimations. The basic input parameters^{3,9-11,13} considered in this design are mentioned in Table 1.

2. DESIGN OVERVIEW AND IMPLEMENTATION

This system requires multiple modules to be designed and get integrated. Two separate channels are considered in this design; one is for low-power laser beam rider (LBR) detection and the other is for both laser range finder (LRF) and laser target designator (LTD). The beam rider laser sensor is comprised of an array of silicon PIN photodiodes arranged in a 4 x 4 matrix. The sensor used for the range finder and designator in the other channel is Excelitas Angular Continuous Threat Detector (EXACTD) from Excelitas². A block diagram of the laser warning sensor is shown in Fig. 2.

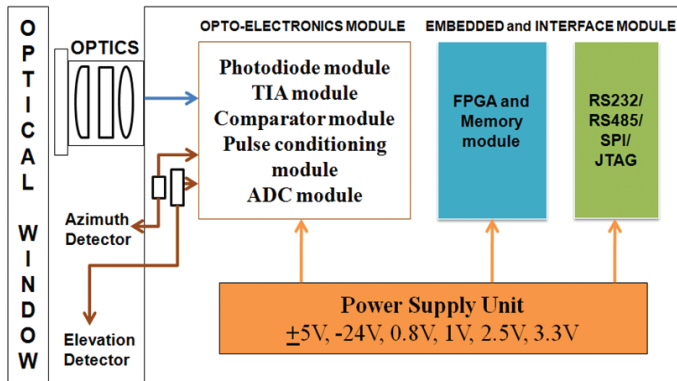


Figure 2. Block diagram of laser warning sensor.

2.1 Received Optical Power Estimation

As discussed in the previous section, there are mainly three types of threats that a target can be vulnerable to exposure. A laser target designator is basically a high-energy laser source along with a programmable pulse repetition frequency. A laser range finder can be used in either a single shot mode or a few multiple pulse modes. A beam rider laser source is a low-power laser with programmable frequency for shorter-distance applications. Initial laser details^{3,6,9-11} required for the estimation of received power density in the sensor plane are taken as mentioned next. Energy level of range finder, designator and beam rider laser considered are 10 mJ, 100 mJ and 0.2 mJ respectively. Beam divergence of range finder, designator and beam rider laser are taken as 0.2 mRad, 0.2 mRad and 2.4 mRad respectively. The laser pulse width is taken as 20 nano second for all three. Considering these as basic input data, an estimation of the received signal at the sensor plane can be calculated by using an equation for atmospheric transmission as given by equation 1. Any optical pulse that travels across an atmospheric channel suffers from losses which can be mainly due to scattering by aerosol particles, absorption by gases, and laser beam divergence.

Received power density in W/cm² can be given by

$$P_d = \frac{4E_t e^{-\sigma d_1}}{\pi(\theta d_2)^2 t_w} \cos(\theta_{AZ}) \cos(\theta_{EL}) \tag{1}$$

Where,

- E_t is transmitted energy in mJ
- σ is atmospheric attenuation coefficient in km⁻¹
- d_1 is atmospheric channel distance in km
- d_2 is total laser travel distance in km
- θ is divergence of laser in mRad
- t_w is pulse width in nanosecond
- θ_{AZ} is obliquity angle of azimuth in deg with input beam
- θ_{EL} is obliquity of elevation in deg with input beam

There can be many scenarios for radiation while traveling through the atmosphere for different visibility conditions. To estimate the available power level, the atmospheric attenuation coefficient is calculated for two visibility conditions of 3 km and 10 km using the Kruse and Kim model^{1,4-5}. For long-range calculation, the atmospheric channel is considered as 5 km while for the minimum range it is the total travel distance only. The maximum range for the range finder and designator is taken as 40 km and for the beam rider, it is considered as 10 km. The minimum range possible for all three threats is taken as 0.5 km. The orientation of the sensor towards the laser source also affects the signal strength. The maximum field of view in azimuth and elevation for the range finder and designator is taken as $\pm 45^\circ$ as per the EXCELITAS sensor details. The Beam rider channel is tested with an available lab optical assembly with a field of view of $\pm 12^\circ$ and the 4 x 4 quadrant detector is used for angular measurement. A theoretical calculation is carried out for different combinations of the target range, visibility condition, and obliquity factors. Accordingly, a summary of maximum and minimum received power density levels is given in Table 2.

Table 2. Calculated power density on sensor plane

Laser type	Minimum power density	Maximum power density	Dynamic range
LRF	0.00978 W/cm ²	5.86 KW/cm ²	57.77 dB
LTD	0.0978 W/cm ²	58.6 KW/cm ²	57.77 dB
LBR	30 μ W/cm ²	4000 μ W/cm ²	21.24 dB

The optics are comprised of a front window with an interference filter for the bands and a combination of multiple lens assemblies for the beam rider channel. Therefore, constructively there is one main optical assembly for the beam rider channel 1 and the two excelitas sensors are placed orthogonally with each other in channel 2.

2.2 Frontend Electronics Module

2.2.1 Laser Beam Rider⁸ Channel

The frontend module of channel 1 comprises 16 photodiodes organized in a square matrix with basic parameters as given below. Each quadrant is made up of four photodiodes and their outputs are joined to get a single current output. As a result, four current output signals are available from the four quadrants. They are converted into voltage output through four

trans-impedance amplifiers (TIA) with programmable gain attached to each amplifier circuit. The TIA outputs are compared with a threshold voltage reference using a comparator amplifier circuit as shown in the figure. This comparison hardware logic detects any laser exposure and generates a Start of Conversion (SoC) signal for further synchronizations. The comparator outputs for each photodiode are also connected to an FPGA bank used for signal acquisition and software processing. The TIA output of each quadrant assembly is converted into digital signals using four separate 8-bit analog-to-digital converters.

The basic parameters of the Si PIN photodiodes are given as follows.

Make	Hamamatsu
Active Area (mm x mm)	10 x 10
Wavelength Range (nm)	400 to 1100
Responsivity (A/W)	0.20 to 0.66
Supply Voltage (V)	-24
Dark Current (nA)	10

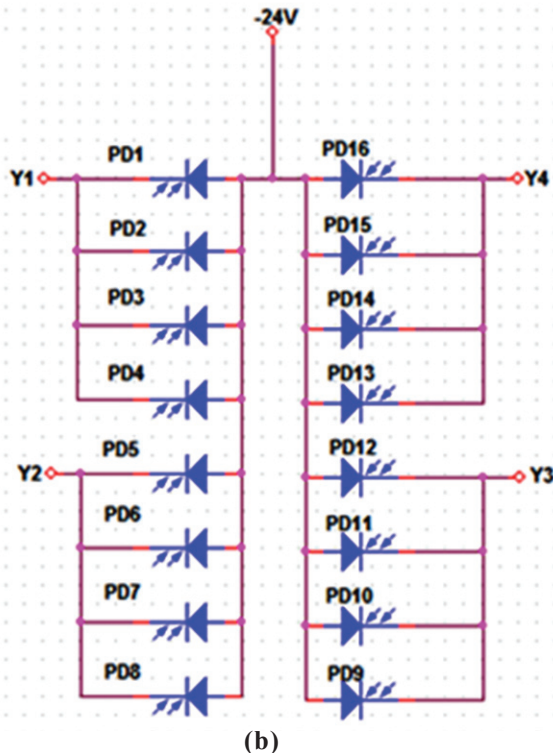
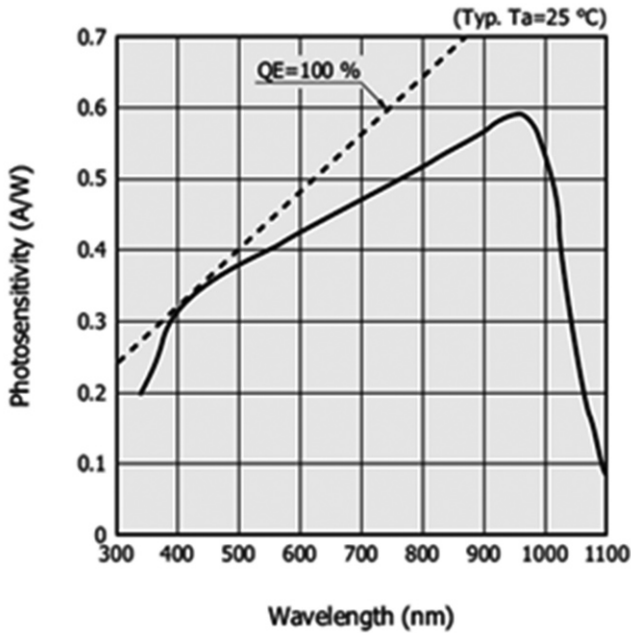


Figure 3. (a) Responsivity curve of Si PIN Photodiode, (b) Photodiode connection details.

The automatic gain control is performed by an FPGA logic through a high-speed switching chip using the i2c protocol. The basic AGC logic is as described in flowchart figure 5 and resistor switches in Fig. 4. First, a calculation is required to decide the AGC resistance values used in the TIA circuit. This calculation is done for minimum and maximum power densities and respective on-axis incidence of radiation and at the maximum angle of incidence respectively.

A typical responsivity curve of a Si PIN photodiode¹² from Hamamatsu is shown in Fig. 3.

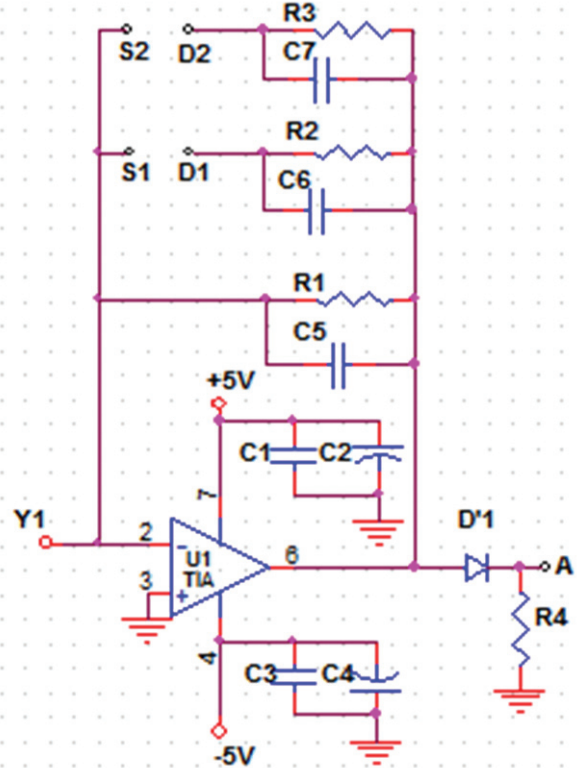


Figure 4. Transimpedance amplifier circuit.

AGC Algorithm of Beam Rider Detector Amplifier:

Diameter of optical aperture stop considered is 35 mm.
 Minimum input power density calculated is $30 \mu\text{W}/\text{cm}^2$
 and Maximum input power density is $4000 \mu\text{W}/\text{cm}^2$.
 Axis parallel radiation power available on detector 15%.
 At maximum angular radiation minimum and maximum overlap are taken as 2 % and 25 % respectively on quadrant active areas based on non-active areas between photodiodes and angle of incidence.

The available power level at the output of aperture stop is (Aperture area) x (Power density).

For minimum input power density:

Power at each quadrant for 0° AoA is 43 μW.

With minimum fractional overlap power on a quadrant for 45° AoA is 5.76 μW.

With maximum fractional overlap power on a quadrant for 45° AoA is 72 μW.

For maximum input power density:

Power at each quadrant for 0° AoA is 5773 μW.

With minimum fractional overlap power on a quadrant for 45° AoA is 770 μW.

With maximum fractional overlap power on a quadrant for 45° AoA is 9621 μW.

Considering the responsivity of the photodiodes as 0.6 A/W from Fig. 3 (a)), the equivalent photocurrents are calculated as given in Table 3.

Table 3. Photo current details of each quadrant

Angle of Arrival on sensor plane	For minimum power density level (30 μW/cm ²)	For maximum power density level (4 mW/cm ²)
0°	25.8 μA	3.5 mA
45° with minimum fractional overlap	3.5 μA	462 μA
45° with maximum fractional overlap	43.2 μA	5.8 mA

Therefore, the dynamic range of the photocurrent is 3.5 μA to 5.8 mA. The comparator reference voltage is taken as 100 mV.

For the initial minimum current, the TIA output should be 100 mV to give the comparator output as high. The resistor value for this voltage would be R1 is 28.57 KΩ.

Assuming a saturation voltage of 2.7 V the current for this voltage would be 95 μA.

Therefore, the current range from 3.5 μA to 95 μA is covered by R1 which is the first feedback resistor. At this current, the first switch should get closed and the TIA voltage level should be lowered to 100 mV. The resistor connected by this switch can be calculated as R2 is 1 KΩ.

Then the current value at saturation voltage of 2.7 V would be 2.7 mA.

Therefore, the current range from 95 μA to 2.7 mA would be covered by the combination of R1 and R2.

Now, at this current level, the second switch should get closed and the voltage level should be lowered to 100 mV again. The resistor connected by the second switch is R3 is 37 Ω.

At saturation, the current would be 73 mA.

Therefore, the current from 2.7 mA to 5.8 mA would be covered by a combination of R1 and R3.

Hence the complete range of current for the full range of input power density levels can be controlled by three programmable feedback resistors bank.

The I²C protocol-based control state machine is implemented in a VHDL code and the flowchart is shown in Fig. 5.

2.2.2 LRF/LTD Channel

The other channel comprises two EXCELITAS sensors

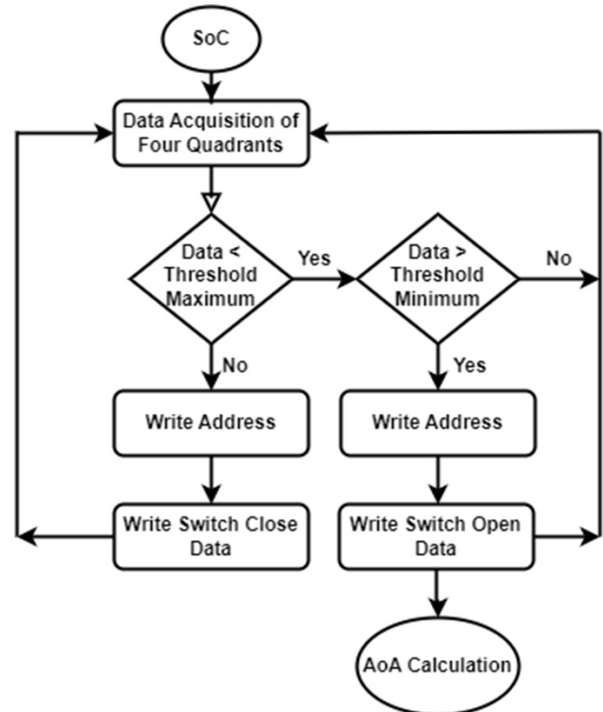


Figure 5. I²C logic for AGC of beam rider detector.

one for azimuth and one for elevation direction both placed perpendicular to each other. The optical passage for these two detectors is through two interference filters one for 1064 nm and the other for 1540 nm center wavelength. Similarly, as the beam rider channel, the EXCELITAS outputs are converted into voltage output using suitable trans-impedance amplifiers and then fed into comparators to get binary outputs. This sensor is made of both Si photodiode as well as InGaS in a masked arrangement to get the broad response band. The photodiode section is masked for both high-sensitivity and low-sensitivity optical elements as per the two photodetector responsivities. The presence of any input radiation can be detected along with the angle of arrival with an accuracy of ±1° with these detectors. The basic specifications of this detector² are given as follows:

Make	EXCELITAS
Active Area (mm ²)	0.075
Wavelength Range (nm)	500 to 1650
Responsivity (A/W)	0.2 to 0.7
Supply Voltage (V)	12
Dark Current (nA)	20
Field of View (deg)	±45°
Angular resolution (deg)	±1°

The responsivity curve² of this sensor is shown in Fig. 6. Some of the bit pattern configurations for this sensor² are shown in Table 4.

Many bit patterns are generated in high-sensitive and low-sensitive channels as per the signal level and responsivity of the sensors. Therefore, different angular information is available from these bit patterns and can be implemented in FPGA logic as described in the next section.

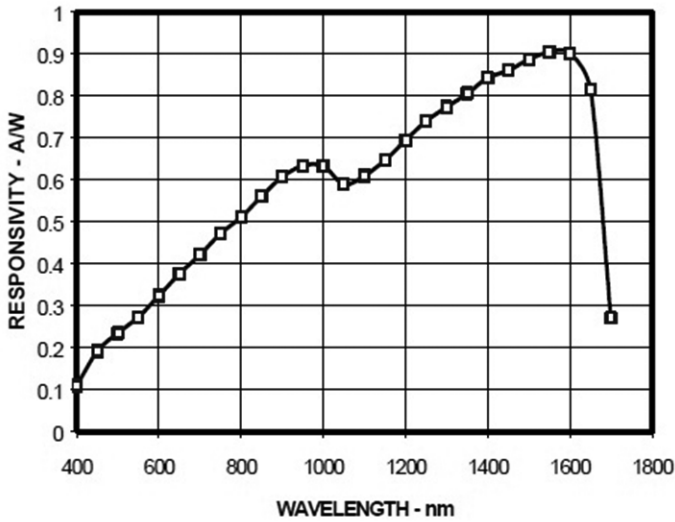


Figure 6. Responsivity curve of broadband photodetector.

Table 4. Output bit pattern and AoA of broadband photodetector

Angle bits	High sensitivity angle (°)	Low sensitivity angle (°)
1 0 0 1 1 1	45.0	38.0
1 0 0 1 0 1	43.6	36.3
1 1 0 1 1 0	13.2	0.8
1 1 0 0 1 0	11.6	-0.7
1 1 0 0 1 1	10.1	-2.3

2.3 Signal Acquisition and Processing in FPGA

As discussed in the previous section, the laser being used in such battlefield applications is of very short pulse and in the range of nanosecond pulse width. The rise time and fall time of such pulses are therefore in sub nanoseconds in time scale. To detect and respond to such a fast pulse FPGA based design is the most versatile and quick one. Also, there is not a single photodiode but quite many photodiodes are being used in this design. Detection of incoming laser pulse by all the photodiodes has to be triggered at the same clock signal that is at the same time. This requires parallel signal processing of all the photodiode channels at the same time. This is possible by executing parallel processes being designed within a single FPGA hardware module.

The processing hardware used in this design has the following basic specifications:

Platform	Xilinx Virtex 5
Clock	100 MHz
Programming Interface	JTAG
Opamp Bandwidth	3.9 GHz
Opamp slew rate	950 V/μsec
ADC sampling rate	1 MSPS
ADC conversion time	660 nsec

The working principle of the laser threat detection system is shown in a flowchart in figure 7 below. This logic is based on basically the pulse repetition frequency of incoming laser pulses.

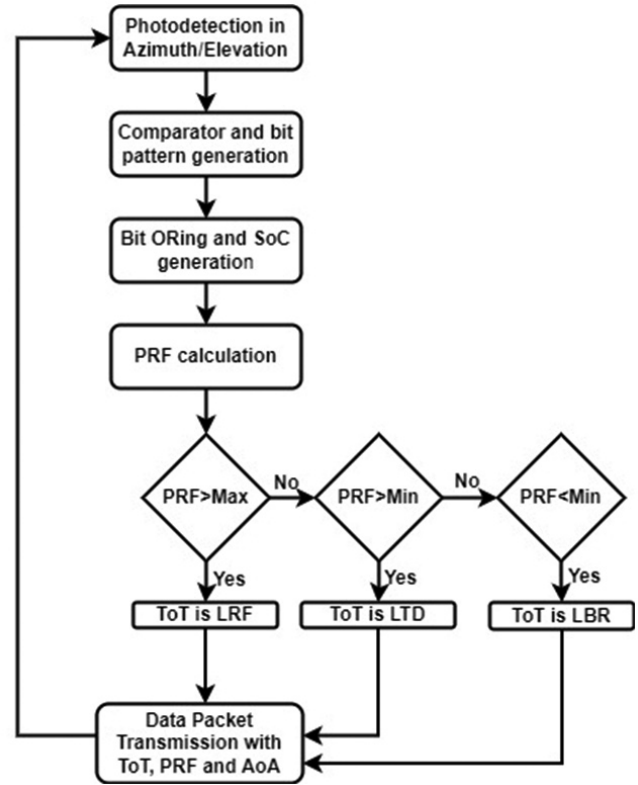


Figure 7. PRF calculation and type of threat logic.

In the beam rider detector design part the incoming radiation is of very low amplitude and has to be detected by the quadrant detector with an array of Si PIN photodiodes arranged as a 4 x 4 matrix in four quadrants as shown in figure 8. Four analog outputs are being generated each combined from four individual photodiodes of each quadrant. Subsequently, these signals are converted to 8-bit signals using four analog-to-digital converters from Analog Devices. Here, the nanosecond pulse being detected is first stretched up to the microsecond level by one opamp circuit to reduce the bandwidth of the signal. This enables the design to use an ADC of lesser sampling speed. The start of ADC conversion is triggered with the help of a Start of Pulse (SoP) being generated by a signal threshold detection circuitry and the ADC control logic is implemented inside FPGA within the VHDL code as shown in Fig. 8.

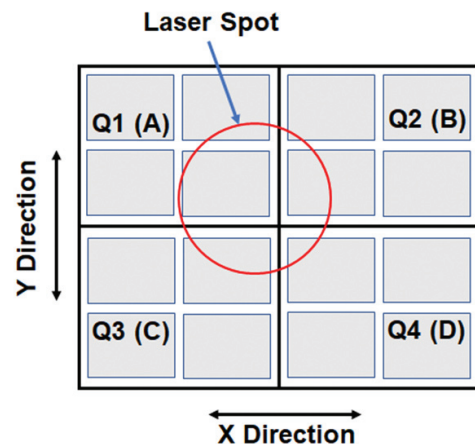


Figure 8. Quadrant detector.

Finally, the angle of incidence is calculated in an FPGA process based on the four quadrant signal difference as shown in Eqn. 2.

$$X = \frac{(B+D)-(A+C)}{A+B+C+D} \tag{2}$$

$$Y = \frac{(A+B)-(C+D)}{A+B+C+D} \tag{3}$$

$$Azimuth = X * (\text{Angular span in x direction}) \tag{4}$$

$$Elevation = Y * (\text{Angular span in y direction}) \tag{5}$$

Table 5. Measured angle of arrival of beam rider detector

Angle change (Deg)	Measured angle (Deg)
-17	-23.5
-16	-22.9
-15	-22.9
-14	-22.1
-13	-21
-12	-19.5
-11	-18.1
-10	-16.2
-9	-13.9
-8	-11.5
-7	-9
-6	-6.9
-5	-5.2
-4	-3.6
-3	-2.3
-2	-1
-1	-0.3
0	0.1
1	0.9
2	1.5
3	3.1
4	4.1
5	5
6	6.1
7	7.8
8	9.3
9	10.1
10	11.3
11	12.8
12	15
13	16.9
14	18.3
15	18.6
16	19.5
17	20

The sensor is placed on a rotational stage and given angular change in an interval of 1° and the angle is measured by the beam rider channel of the sensor. The measured data vs change is given in the figure 9 next. This measurement is done by using one optical assembly available for a field of view of ±12°.

The input angular variation and their measurement done by the sensor prototype is given in Table 5 and a plot is shown in Fig. 9.

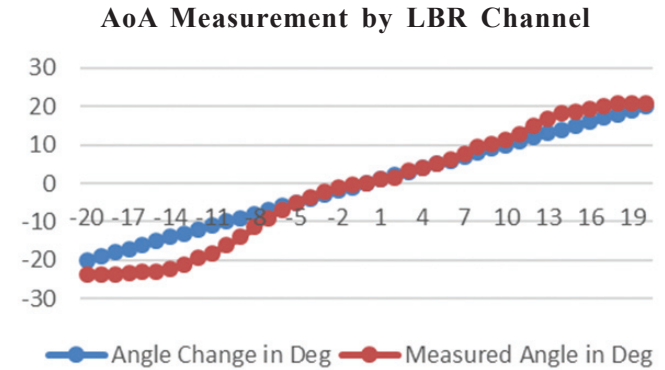


Figure 9. Fired vs measured angle of arrival.

It is seen that with the available optical assembly with a ±12° angular range, a nearly linear response is obtained for this range. Since the divergence of a laser for beam rider projectile is generally large and can be higher than 2 mrad, the angle of incidence can be approximately estimated. To increase the accuracy and range of field of view the number of photodiodes in the array can be increased and the optics also is to be redesigned accordingly.

Long-range high-energy laser sources like range finder and designator pulses are being detected by two broadband EXCALTD detectors as described in previous sections. These two detectors are placed perpendicular to each other one for elevation and the other for azimuth directions. Each of them can resolve the angle of incident radiation up to ±1° for the range of ±45° total field of view. Thus a single such sensor can cover for a 90° full angular coverage. By suitable placement of some such sensors can warn around the platform of deployment.

As far as the implementation is concerned, a lookup table is prepared in the FPGA code for the angle information for both elevation and azimuth direction. As shown in the flowchart Fig. 7, as soon as there is a detection of a laser pulse the processing engine will search for any consecutive pulse. Accordingly, the pulse repetition is observed and the repetition frequency, etc. is calculated. The signal acquisition for this sensor is done similarly as described for the beam rider detector. Here also a set of TIAs are used for each high-sensitive and low-sensitive bit. Subsequently, the TIA outputs are compared with a threshold voltage to generate the bit patterns. The bit patterns are compared from the lookup table to get the specific angle of incidence. The pulse repetition frequency is also calculated with the help of a start of conversion pulse generated by an FPGA process. Now all the required information viz. type of threat, PRF, and angle of arrival are available and they are transmitted to a PC terminal through a serial interface for display purposes. This is enabled by a UART interface circuit

based on RS232 is designed along with the FPGA circuit. The data can be communicated to a master controller which can be designed to acquire data from multiple sensors placed at different positions of an aircraft. The interface for such an onboard sensor network has to be on the 1553 protocol to enhance the military-grade product. The basic circuit design for this system being designed and developed is shown in the Fig. 10.

Complete software is written in VHDL language and the executable code is transferred into the SPI flash memory

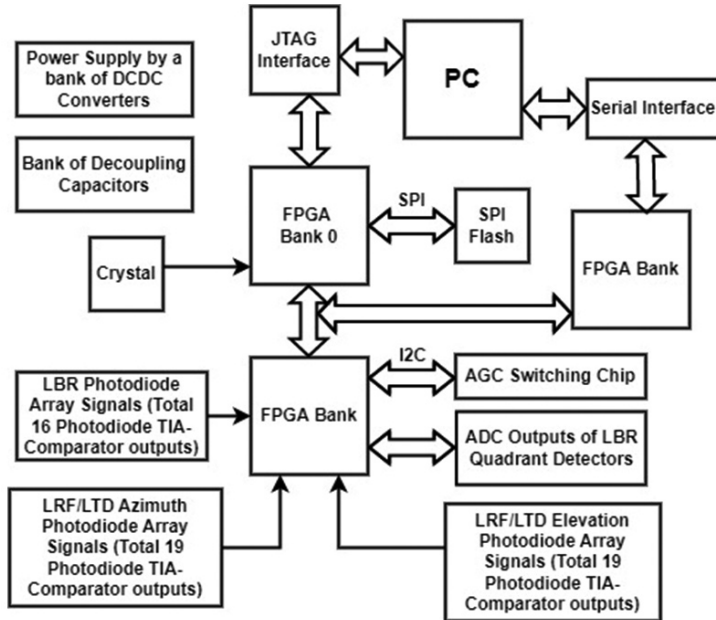


Figure 10. Processing hardware interface.

through the JTAG link being designed as shown in block diagram Fig. 10. Data communication between FPGA and PC for logging and analysis is through a serial interface link as shown. Further, a master controller can be designed based on the 1553 protocol for airborne application. Establishing the exact placement of the laser warning sensors on an airborne platform would require masking analysis through software simulations of platform body structure and their masking on the incoming radiation path. Final outputs for different types of threats viz. range finder, designator, and beam rider with the respective angle of incidence and pulse repetition frequencies are shown in Fig. 11 and Fig. 12 respectively.

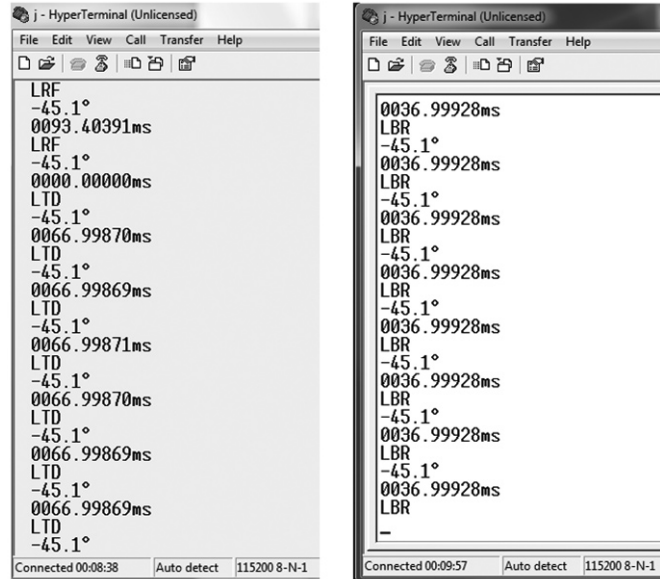


Figure 12. Outputs for designator and beam rider inputs.

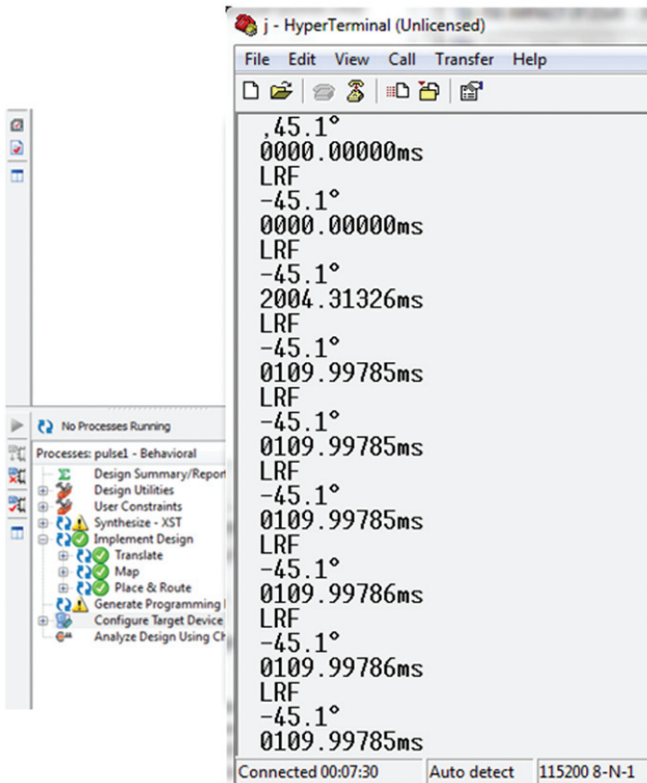


Figure 11. Output for range finder input.

3. RESULTS

The sensor system is tested for multiple exposures to the laser range finder in single shot mode and laser target designator in pulse repetition mode. The Upper and lower limit of pulse repetition time is set in the logic shown in figure 7 as 70 msec and 50 msec respectively. Any laser pulse that is being exposed after 70 msec is considered a type of threat as a range finder and the respective time interval is also measured by the software code. Any laser pulses that are coming with time interval within this range is considered a target designator type of threat. Finally, the laser is fired at a much higher repetition rate for which the time interval is much lesser than 50 msec and the sensor identifies them as a beam rider threat.

The final results of the measured PRF values for different input firing values are summarized in Table 7.

Table 7. Final measured data by the prototype

Type of threat	PRF fired (msec)	PRF measured (msec)	AoA (deg)
LRF	Single Shot/ 110	109.99785	-45.1
LTD	67	66.99869	-45.1
LBR	37	36.99920	-12.0

Pulse repetition frequencies other than those mentioned in the data above, within this range, are being tested with

equivalent accuracies and the type of threat can be predicted accordingly.

4. CONCLUSIONS

In this work, a prototype device has been designed, developed, and tested in the lab for the detection of different types of battlefield laser threats. For airborne application, the design requires further incorporation of other environmental criteria for different conditions. Also, platform masking analysis and placement analysis of sensors for different airborne platforms are required.

5. PSEUDO CODE OF VHDL FOR PRF CALCULATION

```
--Preceded by multiple parallel processes
--VHDL logic of PRF calculation is given
--Diff is the difference between two pulses
process (prf)
--Difftttlakhs
--Difftttlakhs
--Diffttlakhs
--Difftlakhs
--Difflakhs
--Diffthous
--Diffhuns
--Diffpens
--Diffones
begin
if (Diff >= Max) then
LRF <= LRF Flag;
elsif (falling_edge (prf)) then
--Diff, prf is determined in different processes
--Diff is a value and prf is a pulse
LRF <= LRF + 1;
if LRF > 1 then
if Final_Count > Initial_Count then
Diff <= Final_Count-Initial_Count;
else
Diff <=(X- Initial_Count)+Final_Count;
--X is the maximum value of overflow
end if;
else
Diff<= 0;
end if;
Initial_Count <= Final_Count;
for i in 0 to 26 loop
--Shifting part here
case Diffones is
--BCD Conversion Part
end case;
case Diffpens is
--BCD Conversion Part
end case;
case Diffhuns is
--BCD Conversion Part
end case;
case Diffthous is
--BCD Conversion Part
```

```
end case;
case Difflakhs is
--BCD Conversion Part
end case;
case Difftlakhs is
--BCD Conversion Part
end case;
case Diffttlakhs is
--BCD Conversion Part
end case;
case Difftttlakhs is
--BCD Conversion Part
end case;
case Diffttttlakhs is
--BCD Conversion Part
end case;
end loop;
--final shifting part here
end if;
end process;
--Followed by Data formatting part and
--Communication code
```

REFERENCES

1. Naboulsi, Al; Sizun, M.H. & Fornel, de F. Propagation of optical and infrared waves in the atmosphere. France Telecom, 6, Avenue des usines, BP382-90007 BELFORT Cedex, France, 2005
2. EXACTD-362 Angle-of-Arrival Photodiode Module. [https://www.excelitas.com/product/exactd-362-angle-arrival-photodiode-module#:~:text=The%20Excelitas%20EXACTD%20%20%20platform,laser%20Electro%20Optic%20\(E.O.\).](https://www.excelitas.com/product/exactd-362-angle-arrival-photodiode-module#:~:text=The%20Excelitas%20EXACTD%20%20%20platform,laser%20Electro%20Optic%20(E.O.).) (Accessed on 17/07/2019)
3. Maini, N.; Sabharwal, A.; Sareen, K.; Singh A. & Kumar, P. A user programmable electro-optic device for testing laser seekers. *Def. Sci. J.*, 2014, **64**(1), 88-92, doi: 10.14429/dsj.64.4857
4. Sabatini, Capt. R. Tactical laser systems performance analysis in various weather conditions. Italian Air Force Research and Flight Test Division (DASRS), Pomezia 00040 (Rome), Italy, March 1998, TO-MP-001: 29-1 to 29-13
5. Ali, M.A.A. & Ali, A. Performance analysis of fog effect on free space optical communication system. *IOSR J. Appl. Physics*, 2015, **7**(2), 16-24.
6. Gogoi, T.; Kumar, R.; Gladwin, J. & Goyal, V. Testing and evaluation of high energy portable laser source used as a target designator along with a laser seeker. *Def. Sci. J.*, 2018, **68**(5), 494-499. doi: 10.14429/dsj.68.12422
7. Maini, A.K. Battlefield lasers and optoelectronics systems. *Def. Sci. J.*, 2010, **60**(2), 189-196. doi: 10.14429/dsj.60.339
8. Chateaneuf, M.; Lestage, R. & Dubois, J. Laser beam rider hardware-in-the-loop facility. *Electro-optical and infrared systems: Technology and applications II 5987*, 2005, 67-76.

9. Laser System. <https://elbitsystems.com/pdf-category/company-brochures/electro-optics/laser-systems/> (Accessed on 10/08/2023).
10. Laser target designator with laser rangefinder. <https://www.leonardo.us/advanced-targeting-type-163> (Accessed on 10/08/2023).
11. Kumar, S.; Prakash, S.; Maini, A.K.; Patil, V.B. & Sharma, R.B. Design of a laser-warning system using an array of discrete photodiodes-Part II. *J. Battlefield Technol.*, 2011, **14**(2), 13-17.
12. Si photodiodes. <https://www.hamamatsu.com/eu/en/product/optical-sensors/photodiodes/si-photodiodes.html> (Accessed on 07/08/2019).
13. Nejad, S.M.; Arab, H. & Sheshkelani, N.R. Analysis of new laser warning technologies to propose a new optical subsystem. *Iran. J. Electr. Electron. Eng.*, 2018, **14**(3), 213-21.

CONTRIBUTORS

Mr Tutul Gogoi obtained his MTech. in Instrument Technology from IIT, Delhi. He is working at DRDO-DGRE, Chandigarh. He has also experience in the field of target acquisition and tracking technologies for directed energy systems, battlefield laser threat detection, and countermeasure system developments for the protection of high-value assets against laser-guided munitions.

He is responsible for the execution of the task of design of the internal circuit and development of data acquisition and processing software in VHDL.

Ms Rajni Kumar is currently working as a Technical Officer 'D' at the office of the DRDO-Director General, MED CoS. Her research interests are: Development of devices for electro-optically guided precision strike munitions, laser threat detection, and counter measure system developments.

She contributed in the fabrication and testing of the circuits and the complete device.